Comparative Analysis of Hydrogen Vehicle Refueling Dynamics for H35 and H70 Stations at Chilled Temperature (T20)

Antar M. M. Abdala [a], Marco Maggini [b], Misbah Aslam [c] , Stefano Ubertini [d] and Andrea Luigi Facci [e]

[a] *Department of Economics, Engineering, Society and Business Organization, University of Tuscia, 01100 Viterbo, Italy , e-mail*

[b] *Department of Economics, Engineering, Society and Business Organization, University of Tuscia, 01100 Viterbo, Italy , e-mail,*

[c] *Department of Economics, Engineering, Society and Business Organization, University of Tuscia, 01100 Viterbo, Italy , e-mail*

[c] *Department of Economics, Engineering, Society and Business Organization, University of Tuscia, 01100 Viterbo, Italy , e-mail*

[d] *Department of Economics, Engineering, Society and Business Organization, University of Tuscia, 01100 Viterbo, Italy , e-mail, CA*

Abstract:

Hydrogen refueling performance is a critical factor influencing the deployment and user acceptance of fuel cell electric vehicles (FCEVs). This study presents a comparative numerical analysis of hydrogen charging and discharging behavior for H35 (35 MPa) and H70 (70 MPa) refueling stations operating at a chilled temperature of 20 °C (T20). Key parameters, including pressure evolution, mass flow rate, temperature rise, cooling load, hydrogen mass transfer, and state of charge (SOC), are examined under a constant Average Pressure Ramp Rate (APRR) of 5.5 MPa/min. Results indicate that H35 refueling achieves a 50% reduction in charging time compared with H70, primarily due to the lower target pressure and simplified cascade configuration. Temperature rise, cooling demand, and mass flow behavior exhibit similar trends for both systems during the early stages of refueling. The findings provide valuable insights into the thermodynamic and operational characteristics of hydrogen refueling systems, contributing to optimized station design and improved refueling efficiency.

Keywords:

Green hydrogen; Fuel cell electric vehicles; Hydrogen refueling stations; H70 and H35; Chilled temperature T20.

1. Introduction

Hydrogen fuel cell electric vehicles (FCEVs) are increasingly recognized as a promising solution for decarbonizing the transportation sector due to their high efficiency, zero tailpipe emissions, and fast refueling capability. Central to the successful adoption of FCEVs is the development of safe, efficient, and standardized hydrogen refueling infrastructure. Current international standards define two main refueling pressure levels: H35 (35 MPa), typically used for buses and heavy-duty vehicles, and H70 (70 MPa), primarily intended for light-duty passenger vehicles.

Hydrogen refueling involves complex thermodynamics processes, including rapid gas compression, temperature rise due to the Joule–Thomson effect and compression work, heat transfer between hydrogen and tank walls, and dynamic mass flow control through cascade storage systems. Excessive temperature rise during refueling can compromise tank integrity and safety, making thermal management—often through pre-cooled hydrogen—a critical requirement.

This study focuses on a comparative investigation of H35 and H70 refueling stations at a chilled temperature of -20 °C. By analyzing pressure evolution, temperature variations, cooling load requirements, and hydrogen

mass transfer, this work aims to elucidate the operational differences between H35 and H70 systems and provide guidance for infrastructure optimization and energy management.

1.1. Literature review

Significant research has been conducted on hydrogen refueling dynamics, with particular emphasis on thermodynamics, safety, and standard compliance. Melideo et al. investigated fast filling of high-pressure hydrogen tanks and highlighted the dominant role of temperature rise under adiabatic conditions during rapid refueling [1]. Heitsch et al. analyzed the impact of cascade storage configurations on refueling efficiency and demonstrated that optimized cascade sequencing can significantly reduce refueling time and compressor workload [2].

The importance of pre-cooling hydrogen to mitigate temperature rise has been emphasized in several studies. Zhou et al. examined the thermal behavior of on-board hydrogen tanks during fast filling and reported that inlet hydrogen temperature strongly influences maximum gas temperature and state of charge [3]. Similarly, Maus et al. showed that chilled hydrogen refueling is essential for meeting SAE J2601 temperature limits in H70 systems [4].

Rothuizen [5] provided a detailed thermodynamic framework for hydrogen fuelling stations, analyzing the transient behavior of pressure, temperature, and mass flow during vehicle refueling. The study quantified the effects of cascade storage configuration, pressure ramp rate, and pre-cooling on refueling performance and energy demand, establishing key trade-offs between refueling time and thermal constraints.

Comparative analyses between H35 and H70 stations at a chilled temperature of -20 °C remain relatively limited. Reddi et al. evaluated station-level energy consumption and concluded that H70 stations require substantially higher cooling and compression energy compared to H35 systems [6]. Furthermore, ISO 19880-1 provides guidelines on system design and safety requirements for gaseous hydrogen refueling stations, emphasizing controlled pressure ramp rates and thermal management [7].

Building on these prior works, the present study offers a detailed, time-resolved comparison of H35 and H70 refueling performance under identical APRR and chilled conditions, contributing to a more comprehensive understanding of refueling system behavior.

2. Methodology

This study employs a numerical modeling approach to investigate the thermodynamic and operational behavior of hydrogen refueling for H35 and H70 stations at a chilled temperature of -20 °C (T20). The methodology integrates mass, momentum, and energy conservation principles to simulate the dynamic charging and discharging processes of cascade storage tanks and the hydrogen vehicle tank.

2.1. System configuration

The hydrogen refueling station is modeled using a cascade storage system consisting of multiple high-pressure tanks connected in sequence through control valves and a pressure reduction valve (PRV). For the H70 station, four cascade tanks are considered: a tube trailer tank, a low-pressure tank, a medium-pressure tank, and a high-pressure tank, as shown in Fig. 1. In contrast, the H35 station employs a three-stage cascade system, comprising a tube trailer tank, a low-pressure tank, and a medium-pressure tank.

The vehicle hydrogen storage tank is modeled as a fixed-volume, high-pressure composite tank. Hydrogen flows from the cascade tanks to the vehicle tank through a pressure reduction valve, which regulates the inlet pressure according to the prescribed pressure ramp rate.

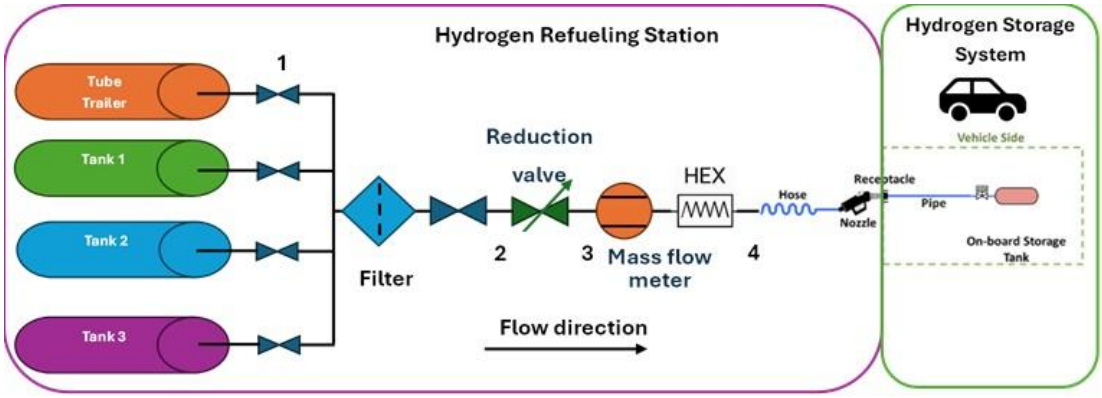

Figure. 1. *HRS under test.*

2.2. Operating conditions and assumptions

The simulations are conducted under standardized refueling conditions consistent with international refueling protocols. The main operating conditions and assumptions are summarized in Table 1 as follows:

Table 1. *Hydrogen refueling station (HRS) parameters and simulation conditions.*

Category	Parameter	Value
Cascade Storage System	Tube Trailer (TT) pressure / volume	20 MPa / 5 m³
	Low-Pressure (LP) tank pressure / volume	33 MPa / 1 m³
	Medium-Pressure (MP) tank pressure / volume	55 MPa / 1 m³
	High-Pressure (HP) tank pressure / volume	90 MPa / 1 m³
Chiller System	Hydrogen pre-cooling temperature	−20 °C
Vehicle Tank	Vehicle tank volume	173 L
	Initial vehicle tank pressure	2 MPa
	Initial hydrogen temperature	300 K
Refueling Protocol	Average Pressure Ramp Rate (APRR)	5.5 MPa/min
	Target pressure (H35)	37.4 MPa
	Target pressure (H70)	72.8 MPa
Thermodynamic Model	Hydrogen property model	Real gas
	Thermophysical properties	Function of pressure and temperature
Heat Transfer Assumptions	Heat transfer to the ambient	Neglected
Flow Modeling	Pipeline pressure losses	Empirical friction correlations
Simulation Conditions	Ambient temperature	25 °C

2.3. Governing equations

The transient refueling process is modeled using a zero-dimensional (lumped-parameter) formulation for both the cascade tanks and the vehicle tank.

2.3.1. Mass conservation

The mass balance for the vehicle tank is expressed as:

$$\frac{dm}{dt} = \dot{m}_{in} \quad (1)$$

where m is the hydrogen mass inside the vehicle tank and $\dot{m}_{in}$is the inlet mass flow rate.

2.3.2. Energy conservation

The energy balance for the vehicle tank is given by:

$$\frac{d(mu)}{dt} = \dot{m}_{in} h_{in} + \dot{Q} \quad (2)$$

where u is the specific internal energy of hydrogen inside the tank, $h_{in}$is the specific enthalpy of the incoming hydrogen, and $\dot{Q}$represents the net heat transfer between the hydrogen and the tank wall and surroundings. In this study, the vehicle tank is assumed to be adiabatic, so $\dot{Q} = 0$.

2.3.3. Equation of state

The mass balance for the vehicle tank is expressed as:

$$P = f(T, \rho) \quad (3)$$

where P is pressure, T is temperature, and ρ is density.

2.4. Cascade tank switching strategy

Refueling begins with hydrogen supplied from the lowest-pressure storage tank (tube trailer). Once pressure equilibrium is reached between the supplying cascade tank and the vehicle tank, the control system switches to the next higher-pressure cascade tank. This sequential switching continues until the target vehicle tank pressure is achieved.

For the H70 station, four cascade stages are activated sequentially, whereas the H35 station utilizes three cascade stages. This switching strategy ensures efficient utilization of stored hydrogen while maintaining the prescribed pressure ramp rate.

2.5. Thermal modeling and cooling load calculation

The thermal behavior of hydrogen during refueling is modeled by accounting for compression heating, Joule–Thomson effects, and heat transfer to the tank wall. The cooling load of the chiller unit is calculated based on the energy required to cool incoming hydrogen after the reduction valve (RV) to −20 °C:

$$\dot{Q}_{cool} = \dot{m}_{in}(h_{RV} - h_{-20°C}) \quad (4)$$

where h_{RV} and $h_{-20°C}$ are the specific enthalpies of hydrogen after the reduction valve and pre-cooled temperatures, respectively.

In this study, the CoolProp library **[8]** is employed to obtain the thermophysical properties of hydrogen**.**

2.6. Performance indicators

The following performance indicators are used to evaluate and compare H35 and H70 refueling systems:

- Charging time
- Pressure evolution in cascade and vehicle tanks
- Hydrogen mass flow rate
- Temperature rise inside the vehicle tank
- Cooling load of the chiller unit
- Hydrogen mass transferred during charging and discharging

- State of Charge (SOC), defined as the ratio of current hydrogen mass to the maximum allowable mass in the vehicle tank.

2.7. Validation

In this study, the HRS simulation is validated against previous work [5]. For this validation, the buffer tank at 90 MPa and the cascade system are compared with the results from [5]. The parameters used for validation include pressure, temperature, mass flow rate, and cooling demand.

The validation of the cascade system is presented in the following figures.

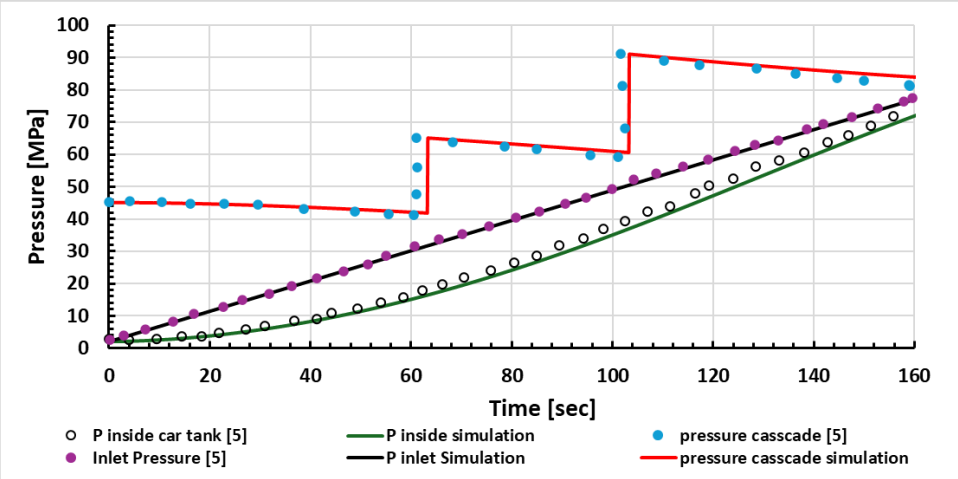

a) Inlet pressure and inside pressure of on-board tank and pressure inside cascade tanks

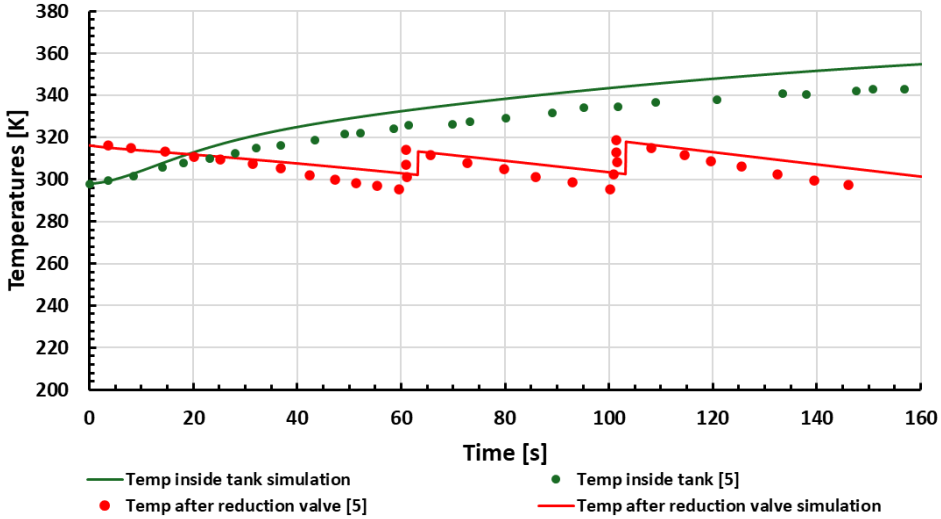

b) temperature inside on-board tank and temperature after reduction valve

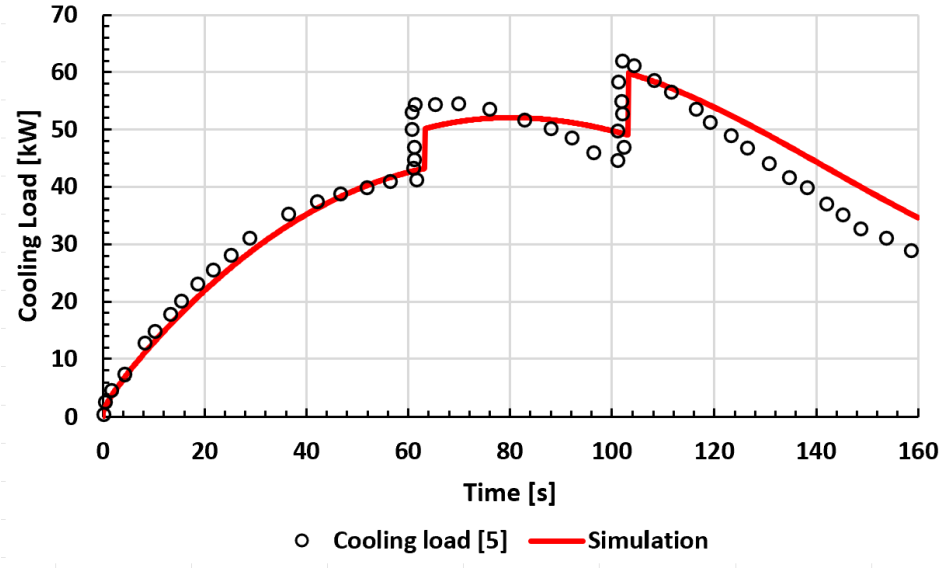

c) *Cooling demand of chiller unit*

Figure. 2. *Validation between other work* ***[5]*** *and simulation for cascade tanks: (a) pressure, (b) temperature, and (c) cooling demand.*

3. Results and Discussion

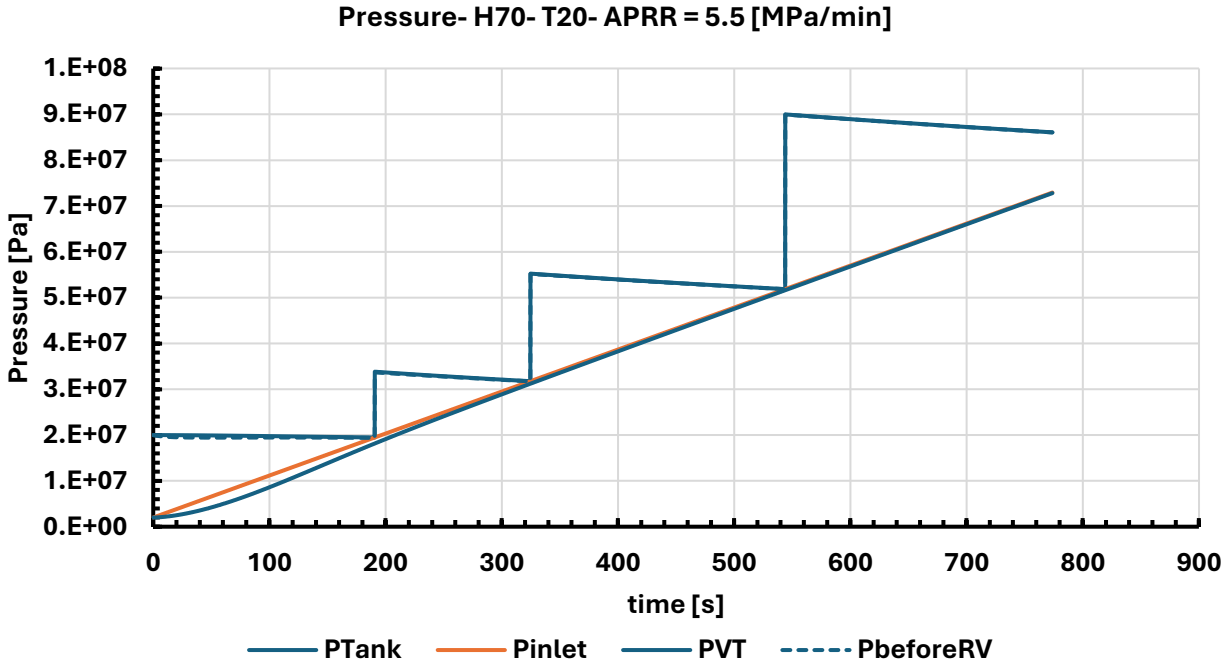

Figure. 3. *Pressure variations during charging and discharging versus time at H70 at T20.*

The Figure 3 illustrates the pressure variations of the cascade storage tanks, the pressure downstream of the pressure reduction valve, and the inlet and internal pressures of the vehicle tank as functions of charging time for H70 at T20.

The discharge pressure from the cascade tanks increases gradually. Assuming an initial vehicle tank pressure of 2 MPa, refueling starts from the tube trailer tank and continues until pressure equilibrium is reached. Subsequently, the low-pressure tank supplies hydrogen to the vehicle tank until equilibrium is again achieved. Thereafter, the third and fourth cascade tanks commence fueling sequentially until the vehicle tank pressure reaches the target value of 72.8 MPa, at which point refueling is terminated.

The inlet pressure increases linearly, following a constant Average Pressure Ramp Rate (APRR) of 5.5 MPa/min. In contrast, the pressure inside the vehicle tank initially increases nonlinearly due to rising mass flow rates, and then transitions to a linear increase, eventually coinciding with the inlet pressure.

The total charging time required for the hydrogen vehicle tank to reach the target pressure of 72.8 MPa is 772.8 s.

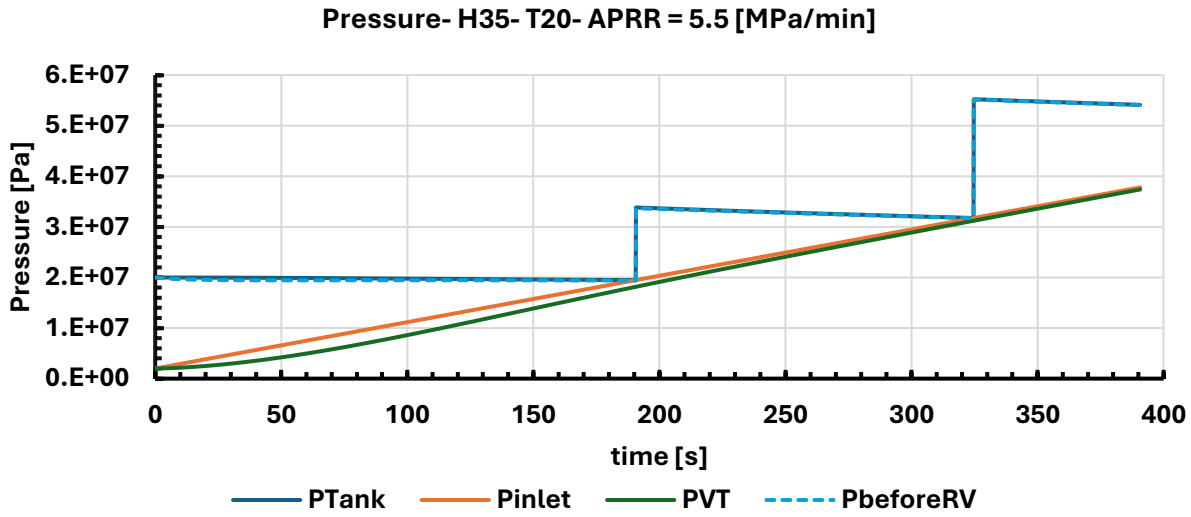

Figure. 4. *Pressure variations during charging and discharging versus time at H30 at T20.*

Figure 4 illustrates the pressure variations of the cascade storage tanks, the pressure downstream of the pressure reduction valve, and the inlet and internal pressures of the vehicle tank as functions of charging time for H35 at T20.

Figure 4 exhibits a similar pressure evolution trend to that observed for H70 (see Fig. 3). However, in this case, the discharge pressure follows a three-stage cascade sequence involving the tube trailer tank, the low-pressure tank, and the medium-pressure tank until the target pressure of 37.4 MPa is achieved.

The total charging time required for the hydrogen vehicle tank to reach the target pressure of 37.4 MPa is 390.7 s, representing approximately a 50% reduction in refueling time compared with the H70 station, which requires 772.8 s.

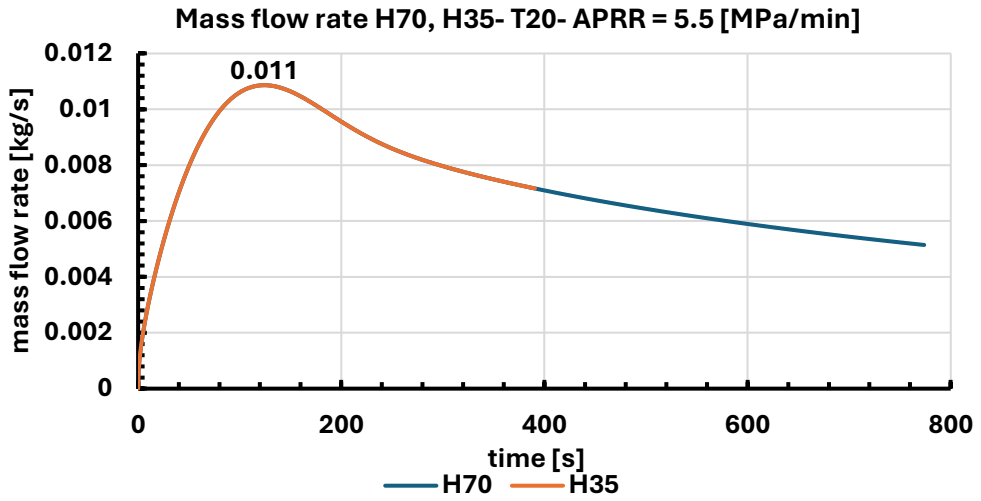

Figure. 5. *Hydrogen mass flow rate during vehicle refueling for H70 and H35 at T20.*

Figure 5 illustrates the variation of hydrogen mass flow rate during the refueling process for H70 and H35 at T20. During charging, the mass flow rate initially increases, reaching a maximum value of 0.011 kg/s at approximately 100 s, and subsequently decreases with time.

It is evident that the total charging time for H35 is shorter than that for H70. The two mass flow rate curves coincide up to 390.7 s, which can be attributed to the identical Average Pressure Ramp Rate (APRR) of 5.5 MPa/min applied in both cases.

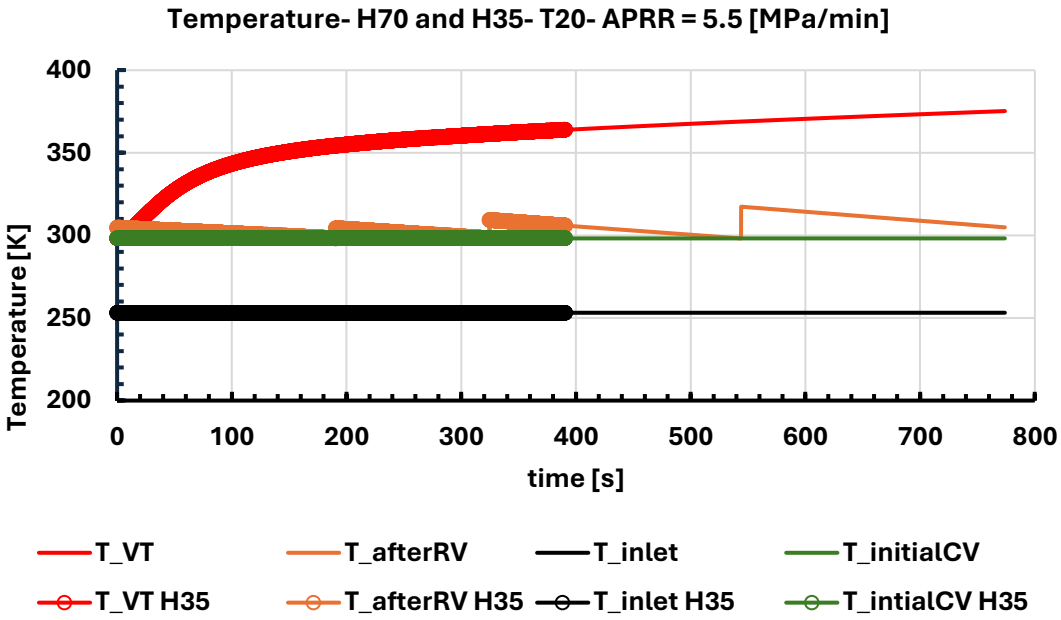

Figure. 6. *temperature variations for H70 and H35 at T20.*

It is evident that the temperature rises rapidly during hydrogen charging, increasing from 300 K to 364 K and 375 K for H35 and H70, respectively, assuming adiabatic conditions, although heat transfer occurs from the hydrogen vehicle tank to the surrounding ambient air.

After passing through the reduction valve, the temperature changes gradually as the pressure increases during discharge from the cascade tanks. The temperature initially rises and then decreases as the pressure drops, primarily due to frictional losses.

During hydrogen charging, we assume a constant chilled temperature of −20 °C. The initial temperature inside the vehicle tank is considered to be 300 K.

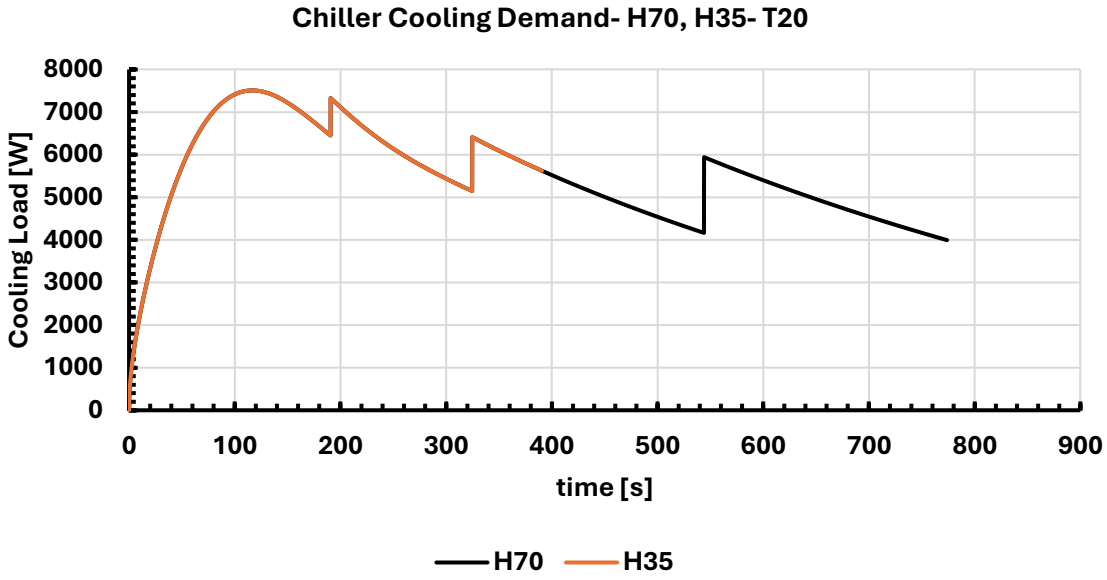

Figure. 7. *Cooling load of chilled unit for H35 and H70 at T20.*

Figure 7 illustrates the variation in cooling load of the chilled unit required to cool hydrogen to −20 °C for H35 and H70. Both H35 and H70 exhibit a high initial cooling demand of approximately 7400 W between 130 and 150 s, which gradually decreases over time. Distinct drops in the cooling load are observed in both curves, corresponding to the switching between cascade tanks and pressure adjustments via reduction valves. These variations reflect the dynamic interplay between tank pressure, temperature, and heat transfer within the chiller system.

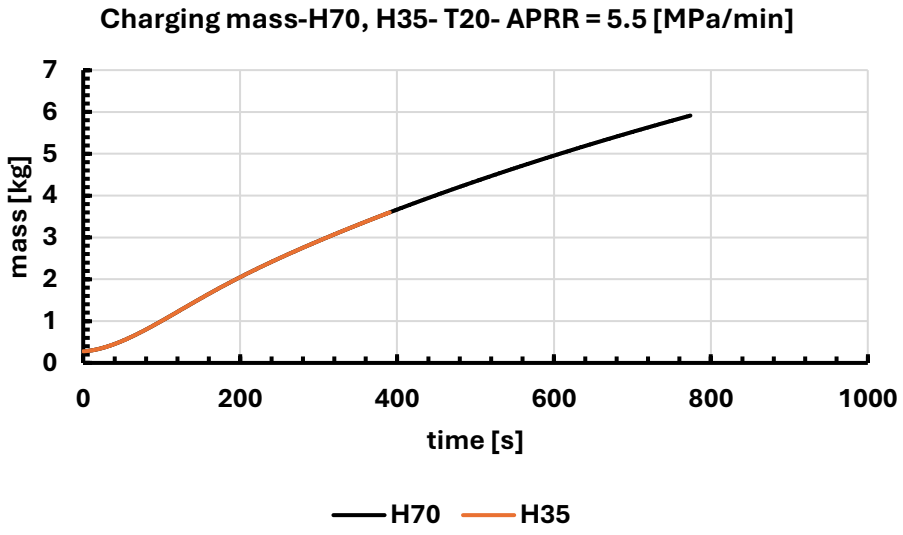

Figure. 8. *Hydrogen charging mass for H35 and H70 at T20.*

Figure 8 depicts the variation of hydrogen charging mass over time for H35 and H70 at T20. The hydrogen mass increases during charging until the target pressure is reached, attaining approximately 3.6 kg for H35 and 5.9 kg for H70.

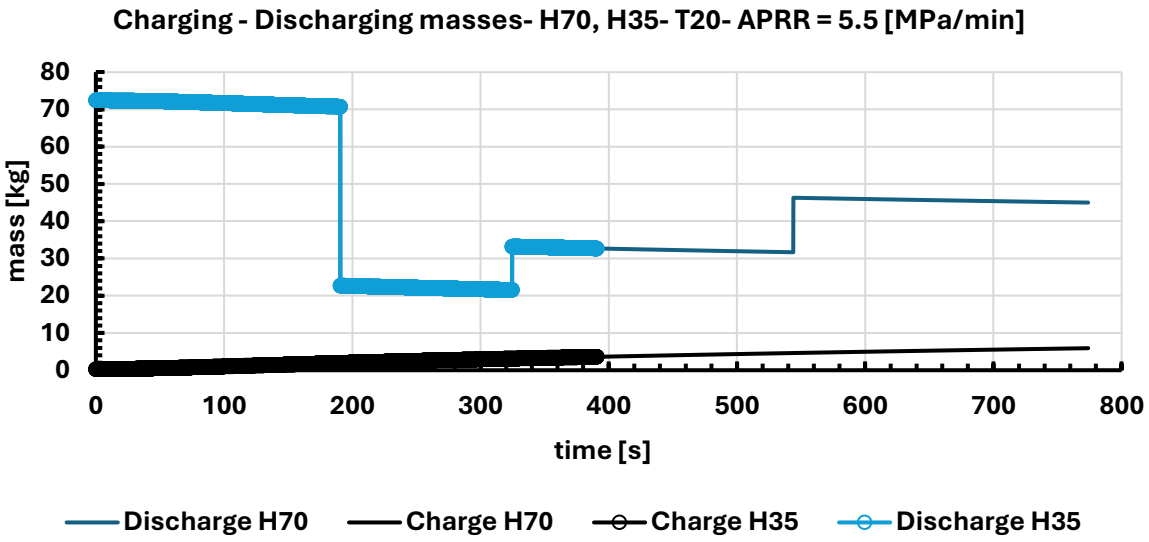

Figure. 9. *Discharge cascade and charge hydrogen masses for H35 and H70 at T20.*

Figure 9 shows the variation of hydrogen mass during charging and discharging for H70 and H35 at T20.

During **discharge**, both H70 and H35 exhibit rapid, stepwise decreases in mass. H70 and H35 start at 72 kg and decrease in stages, with these sudden reductions corresponding to sequential tank operations and pressure relief events.

During **charging**, the mass of hydrogen increases gradually over time. H70 rises from near zero to about 7 kg, while H35 increases to approximately 4 kg. The gradual nature of these curves reflects a controlled charging process, in contrast to the abrupt discharging steps.

Overall, the stepwise discharges combined with the gradual charging highlight the dynamic interplay between tank pressure, heat transfer, and valve operations. This figure effectively illustrates the asymmetric behavior of charging versus discharging in hydrogen storage systems, emphasizing important operational considerations for system design and safety.

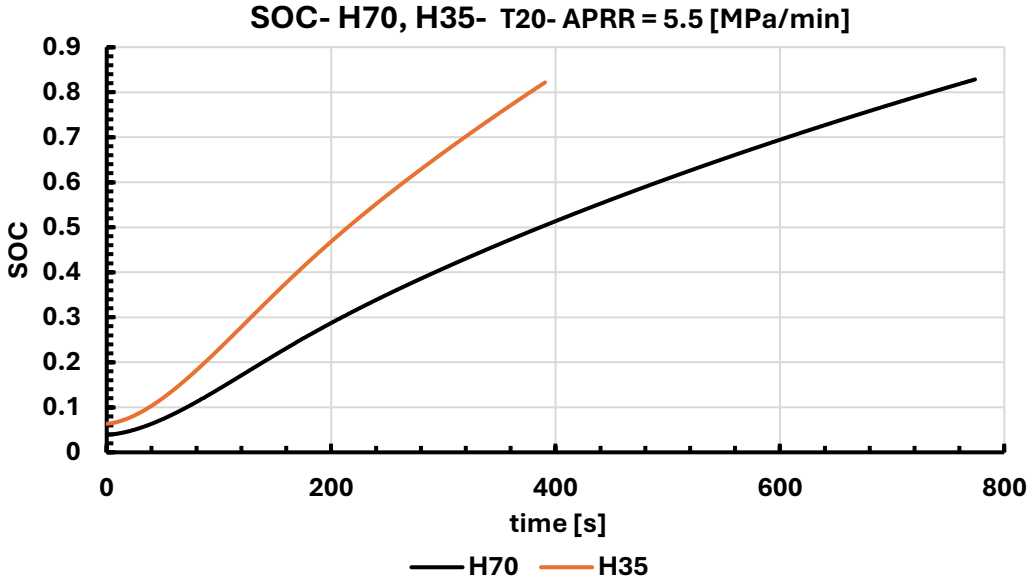

Figure. 10. *State of Charge (SOC) for H35 and H70 at T20.*

Figure 10 shows the variation of the state of charge (SOC) for H35 and H70 at T20. The SOC increases over time until the pressure in the vehicle tank reaches the target pressure. The maximum SOC for both H35 and H70 at T20 is approximately 82%.

4. Conclusion

This study presented a comparative analysis of hydrogen refueling dynamics for H35 and H70 stations at a chilled temperature of -20 °C under a constant APRR of 5.5 MPa/min. The results demonstrate that while both refueling systems exhibit similar pressure, mass flow, and thermal trends during the early stages of charging, significant differences arise due to the target pressure and cascade configuration.

The H35 station achieves the target pressure of 37.4 MPa in 390.7 s, approximately half the refueling time required by the H70 station, which reaches 72.8 MPa in 772.8 s. Temperature rise within the vehicle tank is more pronounced for H70, leading to higher peak temperatures and increased cooling load requirements. Despite these differences, both systems show comparable initial cooling demands due to identical pressure ramp rates.

The stepwise discharge behavior of cascade tanks and the gradual charging of the vehicle tank highlight the asymmetric nature of hydrogen transfer processes. Overall, the findings underscore the trade-offs between refueling speed, thermal management, and energy consumption in H35 and H70 systems. These insights can support improved design, control strategies, and energy optimization of future hydrogen refueling infrastructure.

Acknowledgments

This project has been partially supported by the projects:

• PRIN P20223JMB3 - Modeling and optimization of sustainable hydrogen refueling infrastructures (HyREFI) and PRIN 2020BFX8JY - Hybrid Sustainable Mobil-ity (HYSUM).

• ECS 0000024 Rome Technopole, CUP B83C22002820006, National Recovery and Resilience Plan (NRRP) Mission 4 Component 2 Investment 1.5, funded by the European Union-NextGenerationEU.

• National Recovery and Resilience Plan (NRRP), Mission 4 Component 2 Investment 1.3 - Call for tender No. 1561 of 11.10.2022 of Ministero dell'Università della Ricerca (MUR); funded by the European Union-NextGenerationEU.

Nomenclature

Symbol	Description	Unit
APRR	Average pressure ramp rate	MPa·min⁻¹
(h_{in})	Specific enthalpy of inlet hydrogen	J·kg⁻¹
(h_{RV})	Specific enthalpy after reduction valve	J·kg⁻¹
(h_{-20})	Specific enthalpy at −20 °C	J·kg⁻¹
(m)	Hydrogen mass inside vehicle tank	kg
($\dot{m}$)	Inlet hydrogen mass flow rate	kg·s⁻¹
(P)	Pressure	MPa
($\dot{Q}$)	Heat transfer rate	W
$\dot{Q}_{Cool}$	Cooling load of chiller unit	W
SOC	State of charge	%
(t)	Time	s
(T)	Temperature	K
(u)	Specific internal energy of hydrogen	J·kg⁻¹
(V)	Tank volume	m³ or L
(ρ)	Hydrogen density	kg·m⁻³

References

[1] Melideo, D., Baraldi, D., Acosta-Iborra, A., & Cebolla, R. (2017). *Thermal effects during fast filling of hydrogen vehicle tanks*. International Journal of Hydrogen Energy, 42(8), 5326–5338.

[2] Heitsch, M., Wiedemann, J., & Müller, S. (2015). *Optimization of cascade storage systems for hydrogen refueling stations*. International Journal of Hydrogen Energy, 40(35), 11452–11460.

[3] Zhou, J., Zhao, L., & Li, Y. (2019). *Numerical investigation of temperature rise in on-board hydrogen tanks during fast filling*. Applied Thermal Engineering, 150, 1213–1223.

[4] Maus, S., Hapke, J., Na Ranong, C., Wüchner, E., & Friedlmeier, G. (2008). *The Joule–Thomson effect for hydrogen refuelling*. International Journal of Hydrogen Energy, 33(15), 4137–4146.

[5] Rothuizen, E. D. (2013). *Hydrogen fuelling stations: A thermodynamic analysis of fuelling hydrogen vehicles for personal transportation* (PhD's thesis). Technical University of Denmark, Department of Mechanical Engineering.

[6] Reddi, K., Elgowainy, A., Rustagi, N., & Gupta, E. (2017). *Impact of hydrogen refueling station design on energy use and cost*. International Journal of Hydrogen Energy, 42(39), 24816–24828.

[7] ISO 19880-1. (2020). Gaseous hydrogen—Fueling stations—Part 1: General requirements. International Organization for Standardization.

[8] Ian H. Bell, Jorrit Wronski, Sylvain Quoilin, and Vincent Lemort,"Pure and Pseudo-pure Fluid Thermophysical Property Evaluation and the Open-Source Thermophysical Property Library CoolProp," Industrial & Engineering Chemistry Research, 2014, 53(6), pp. 2498–2508. https://doi.org/10.1021/ie4033999